



ORIGINAL ARTICLE

Morphometric imaging and quantitative susceptibility mapping as complementary tools in the diagnosis of parkinsonisms

Sonia Mazzucchi¹ | Eleonora Del Prete² | Mauro Costagli^{3,4} | Daniela Frosini² |
Davide Paoli¹ | Gianmichele Migaletto⁵ | Paolo Cecchi⁵ | Graziella Donatelli^{5,6}  |
Riccardo Morganti⁷ | Gabriele Siciliano¹ | Mirco Cosottini^{6,8} | Roberto Ceravolo^{1,9} 

¹Neurology Unit, Department of Clinical and Experimental Medicine, University of Pisa, Pisa, Italy

²Neurology Unit, Department of Medical Specialties, Azienda Ospedaliero-Universitaria Pisana, Pisa, Italy

³Department of Neuroscience, Rehabilitation, Ophthalmology, Genetics, Maternal and Child Sciences (DINOGLI), University of Genoa, Genoa, Italy

⁴Laboratory of Medical Physics and Magnetic Resonance, IRCCS Stella Maris Foundation, Pisa, Italy

⁵Neuroradiology Unit, Azienda Ospedaliero-Universitaria Pisana, Pisa, Italy

⁶Imago7 Research Foundation, Pisa, Italy

⁷Section of Statistics, University Hospital of Pisa, Pisa, Italy

⁸Neuroradiology Unit, Department of Translational Research and New Technologies in Medicine and Surgery, University of Pisa, Pisa, Italy

⁹Centre for Neurodegenerative Diseases, Parkinson's Disease and Movement Disorders, Azienda Ospedaliero-Universitaria Pisana, Pisa, Italy

Correspondence

Roberto Ceravolo, Centre for Neurodegenerative Diseases, Parkinson's Disease and Movement Disorders, Azienda Ospedaliero-Universitaria Pisana, Building 13, Santa Chiara Hospital, Via Roma 67, 56126 Pisa, Tuscany, Italy.
Email: roberto.ceravolo@unipi.it

Abstract

Background and purpose: In the quest for in vivo diagnostic biomarkers to discriminate Parkinson's disease (PD) from progressive supranuclear palsy (PSP) and multiple system atrophy (MSA, mainly p phenotype), many advanced magnetic resonance imaging (MRI) techniques have been studied. Morphometric indices, such as the Magnetic Resonance Parkinsonism Index (MRPI), demonstrated high diagnostic value in the comparison between PD and PSP. The potential of quantitative susceptibility mapping (QSM) was hypothesized, as increased magnetic susceptibility ($\Delta\chi$) was reported in the red nucleus (RN) and medial part of the substantia nigra (SNImed) of PSP patients and in the putamen of MSA patients. However, disease-specific susceptibility values for relevant regions of interest are yet to be identified. The aims of the study were to evaluate the diagnostic potential of a multimodal MRI protocol combining morphometric and QSM imaging in patients with determined parkinsonisms and to explore its value in a population of undetermined cases.

Method: Patients with suspected degenerative parkinsonism underwent clinical evaluation, 3 T brain MRI and clinical follow-up. The MRPI was manually calculated on T1-weighted images. QSM maps were generated from 3D multi-echo T2*-weighted sequences.

Results: In determined cases the morphometric evaluation confirmed optimal diagnostic accuracy in the comparison between PD and PSP but failed to discriminate PD from MSA-p. Significant nigral and extranigral differences were found with QSM. RN $\Delta\chi$ showed excellent diagnostic accuracy in the comparison between PD and PSP and good accuracy in the comparison of PD and MSA-p. Optimal susceptibility cut-off values of RN and SNImed were tested in undetermined cases in addition to MRPI.

Conclusions: A combined use of morphometric imaging and QSM could improve the diagnostic phase of degenerative parkinsonisms.

KEYWORDS

brain MRI, morphometric indexes, parkinsonisms, quantitative susceptibility mapping

This is an open access article under the terms of the [Creative Commons Attribution-NonCommercial](https://creativecommons.org/licenses/by-nc/4.0/) License, which permits use, distribution and reproduction in any medium, provided the original work is properly cited and is not used for commercial purposes.

© 2022 The Authors. *European Journal of Neurology* published by John Wiley & Sons Ltd on behalf of European Academy of Neurology.

INTRODUCTION

Early differential diagnosis between Parkinson's disease (PD) and other degenerative parkinsonisms can be challenging, despite the improvement of clinical diagnostic criteria [1–3]. The clinical presentation of PD may overlap with that of multiple system atrophy (MSA, predominantly the parkinsonian phenotype MSA-p) and progressive supranuclear palsy (PSP), limiting the development of disease-modifying treatments [4].

Many advanced magnetic resonance imaging (MRI) techniques have been tested [5, 6] to improve the contribution of imaging to assessment of patients with parkinsonism. Morphometric MRI first demonstrated the selective atrophy of brainstem and cerebellar structures in PSP and MSA but not in PD patients. These measures were then combined in morphometric indices to further increase their diagnostic accuracy [7–10], even though there was some inconsistency between studies [11]: the pons-to-midbrain ratio (P/M) and the Magnetic Resonance Parkinsonism Index (MRPI) demonstrated similar high diagnostic potential in the differential diagnosis between PD and PSP, mainly with regard to Richardson's syndrome (PSP-RS). Decision tree models combining different brainstem-derived MRI planimetric measures yielded high diagnostic accuracy for the discrimination of PSP patients from early clinically uncertain stages [12], and morphometric indices seem capable of predicting the evolution of undetermined parkinsonisms toward PSP [13] also early in the disease course, when patients have a clinically unclassifiable neurodegenerative parkinsonism [14].

Although an overlap at individual level between PD, PSP and MSA patients has been reported, both the MRPI and P/M were included amongst level 2 neuroimaging tools to support the clinical diagnosis of PSP-RS and hypothesized to reach level 3, as early diagnostic biomarkers [15]. Nevertheless, midbrain atrophy is highly variable across PSP phenotypes and disease stages [15–18], and is more evident in patients with PSP-RS and frontal variants, followed by other variants and PSP-parkinsonism (PSP-p) [19]. Despite a pooled 96% sensitivity and 98% specificity of the MRPI in differentiating PSP from PD [20], this variability explains the suboptimal diagnostic accuracy obtained when morphometric indices were used to compare PD subjects and patients affected by PSP-p and PSP variants (PSP-v) [21]. Based on a large multicentre study, the MRPI value of 13.42 was proposed as the optimal cut-off for early differential diagnosis between PSP and non-PSP cases with an accuracy of 88.3% [22]. In contrast, both MRPI and midbrain to pons ratio showed suboptimal diagnostic value in distinguishing PSP from MSA patients [12, 23]. The MRPI is a time-consuming index but was hypothesized to be less influenced by age compared to P/M [24], even though the influence of gender and age was not confirmed in a large cohort of healthy controls [25].

Regional atrophy could be considered a late radiological biomarker and MRI techniques targeting microstructural changes in regions of interest (ROIs), such as iron-sensitive sequences, have been explored. The qualitative assessment of the substantia nigra (SN) significantly improved the differential diagnosis between degenerative

and non-degenerative parkinsonisms [26–32], and encouraging results support the value of quantitative susceptibility mapping (QSM) in discriminating between degenerative parkinsonisms [33–35]. Compared to PD, increased magnetic susceptibility was reported in the midbrain of PSP patients, mainly in the red nucleus (RN), and in the putamen of MSA patients [35]. The identification of disease-specific susceptibility cut-off values could improve the diagnostic potential of QSM, in addition to newly available automated techniques for the segmentation of deep brain nuclei [36]. Although QSM has been widely applied in PD patients [37–41] and in different disease stages [40], a large variability of regional susceptibility values has been reported [42], possibly related to the heterogeneity of the methods applied across studies. The combined use of morphometric and QSM methods was recently hypothesized to add diagnostic value to the differential diagnosis between PD and PSP [43].

The primary aim of the present study was to use multimodal brain MRI to evaluate the diagnostic accuracy of morphometric imaging and QSM in patients with a clinical diagnosis of PD, MSA or PSP at the time of the MRI, calculating optimal disease-specific cut-off values of the most accurate QSM variables.

The secondary aim was to explore the diagnostic value of a combined imaging protocol including QSM and morphometric measures (MRPI) in a population of clinically undetermined parkinsonisms at the time of the MRI, clinically assessed over time until a diagnosis of PD, MSA or PSP was made.

METHOD

Study group

From 2016 to 2019, consecutive outpatients with suspected degenerative parkinsonism were evaluated at the Movement Disorders Centre of Pisa University and were followed over time.

At baseline each subject underwent a clinical evaluation by a neurologist with experience in movement disorders and, within 2 weeks, a 3 T MRI of the brain.

Current clinical diagnostic criteria for PD, MSA and PSP were applied to each subject [1–3]. For PSP patients recruited before 2017, clinical diagnosis was revised according to the Movement Disorder Society (MDS) criteria [2].

Patients fulfilling a clinical diagnosis of possible/probable PD, MSA or PSP at baseline were included in the 'determined' cases group and inter-group radiological differences were investigated. All the remaining cases with clinical evidence of cardinal signs of parkinsonism of any severity but not fulfilling current diagnostic criteria for PD, MSA or PSP were defined as 'undetermined'. Diagnosis was reviewed on annual clinical follow-up.

Patients with MSA were categorized into MSA-p and cerebellar MSA (MSA-c) phenotypes. MSA-c cases were included because they present parkinsonian signs in the early stages, according to the neuropathological model of the disease [44]. In patients with possible/probable PSP, the clinical phenotype was defined and reviewed

annually according to the multiple allocations extinction criteria [45]. Given the limited number of subjects classified as PSP-p or PSP-v, the natural history of the disease and the prospective design of the study, all PSP cases were analysed as a single group.

Patients with undetermined parkinsonism at baseline ('undetermined cases') underwent clinical follow-up until each subject fulfilled clinical diagnostic criteria for PD, MSA or PSP [1–3]. The diagnostic doubt at baseline was recorded.

The following data were recorded at baseline: demographic data, disease duration, levodopa equivalent daily dose (in subjects with baseline ongoing treatment), motor assessment with sub-score III of the Unified Parkinson Disease Rating Scale (UPDRS, OFF-state) [46] and the PSP Rating Scale [47] in PSP patients and the clinical phenotype in PD subjects (tremor dominant or postural instability gait disorder) [48]. The Movement Disorder Society clinical diagnostic criteria for 'clinically established early PD' were further applied [49]. The presence of typical rest tremor or red flags was investigated. Recordings included the evaluation of response to dopaminergic treatment (when applicable), the presence of dyskinesia and/or fluctuations, asymmetry of parkinsonism, orthostatic hypotension, urinary dysfunction and the presence of the PSP core clinical features (i.e., ocular motor dysfunction, postural instability and akinesia with levels of certainty 1–3) [3].

Exclusion criteria were concomitant neurodegenerative disorders, claustrophobia/contraindications to MRI, cognitive impairment affecting the understanding of informed consent or interfering with imaging acquisition, and relevant white matter lesion load measured by the age-related white-matter changes score (patients with score >2 were excluded).

The study was conducted according to ethical standards and approved by the local ethics committee. All participants gave written informed consent.

Imaging protocol

The MRI acquisitions were performed on an MR750 3 T scanner (GE Healthcare, Chicago, USA); the protocol included a 3D T1-weighted sequence (repetition time [TR] 8.2 ms, inversion time [TI] 450 ms, echo time [TE] 3.2 ms, flip angle [FA] 12°, spatial resolution $1 \times 1 \times 1 \text{ mm}^3$) and a 3D multi-echo T2*-weighted sequence (TR = 66.7 ms, TE1:ΔTE:TE16 = 13:3.3:62.5 ms, FA = 15°, number of excitations 0.70, spatial resolution $0.93 \times 0.93 \times 1 \text{ mm}^3$, prescribed axially). The magnitude and phase of the complex data were processed, and an average T2*-weighted 3D image and one quantitative magnetic susceptibility (χ) map were generated for each patient following phase unwrapping, background phase removal and dipole inversion, according to an established processing route [50].

The morphometric indices P/M and MRPI were manually calculated on T1-weighted images, according to published methodology [10]. For MRPI, the formula (P/M) \times (medium cerebellar peduncle width/superior cerebellar peduncle width) was employed and a cut-off of 13.42 was applied to all cases [22].

For the susceptibility evaluation, ROIs were manually drawn on QSM maps on the following regions: SN sub-compartments SNImed, SNllat, SNllventr, SNllint, SNlldors (following an established protocol) [27], RN, subthalamic nucleus (STN), globus pallidus, caudate and putamen, on both sides of each patient [35]. Relative susceptibility values ($\Delta\chi$) for each ROI of each side were computed as the difference between the mean χ value of each ROI and the mean χ value of a reference ROI (RR) drawn in the sub-cortical white matter of the right occipital lobe, in accordance with a previously described procedure [35]. An average $\Delta\chi$ value of each region, expressed in parts per billion (ppb), was then obtained as an average of $\Delta\chi$ of both sides in each patient.

Statistics

The normal distribution of all continuous variables was evaluated with Shapiro–Wilk and Kolmogorov–Smirnov tests. Two of the continuous variables (disease duration and susceptibility values of the SN) were not normally distributed and therefore only non-parametric tests were used for data analysis. Continuous data are described by median and interquartile range (IQR).

To compare clinical and radiological continuous factors with clinical groups, the Kruskal–Wallis test and Mann–Whitney test were used. Bonferroni's correction was applied to pairwise comparisons.

To investigate the effect of age on radiological variables the Mann–Whitney test was first applied, followed by multiple linear regression modelling using disease group and age as independent variables and susceptibility values as dependent variable; in this way the differences related to the disease were adjusted for age. Any significant effect of gender regarding all continuous variables was investigated.

Finally, to evaluate the diagnostic accuracy of morphometric and quantitative variables the area under the curve of the receiver operating characteristic (ROC) was calculated. The diagnostic performance of each variable to allocate patients to the diagnostic groups was considered as follows: excellent, area under the ROC curve (AUROC) 0.90–1.00; good, AUROC 0.80–0.89; fair, AUROC 0.70–0.79; poor, AUROC 0.60–0.69; or fail, AUROC 0.50–0.59. The significance level was set to 0.05 and all statistical analyses were carried out with IBM SPSS v.27.

RESULTS

Clinical evaluation

Baseline

A total of 111 patients, who underwent clinical and radiological evaluation at baseline, were included in the study. The median age of the entire population was 68 (IQR 60–73), disease duration was 3.0 years (IQR 2.0–5.0), UPDRS III was 25 (IQR 14–32) and levodopa equivalent daily dose was 300 (IQR 116.2–621.2).

In 69/111 cases (62%) the baseline clinical evaluation led to a diagnosis of PD (31), MSA (14, five MSA-p and nine MSA-c) or PSP (24, 16 PSP-RS, five PSP-p and three PSP-v; early supranuclear gaze palsy [level of certainty 1] was recorded in 11 cases and early postural instability [level of certainty 1] in 17). PD patients were classified according to the clinical phenotype: 17 were postural instability gait disorder, 10 were tremor dominant and four had a mixed phenotype. The diagnosis of clinically established early PD was fulfilled in 60% of PD cases; early motor complications were recorded in three cases.

Forty-two out of 111 patients (38%) were classified as undetermined cases. The differential diagnostic doubt recorded at baseline was 'PD or PSP?' ($n = 23$) and 'PD or MSA-p?' ($n = 19$).

Clinical details of determined and undetermined cases are summarized in Table 1 and Table S1.

Follow-up

Median clinical follow-up of the population was 26 months (IQR 14–38). The baseline clinical diagnosis was confirmed as the final diagnosis in all the determined cases (31 PD, five MSA-p, nine MSA-c, 24 PSP). All the undetermined cases were classified within the observational period and the final clinical diagnoses were 13 PD, eight MSA-p, 21 PSP.

Radiological evaluation

Morphometric evaluation was possible in all patients whereas QSM images were available in 99/111 (89%) cases, 60 determined and 39 undetermined. In the remaining subjects, either severe

motion artefacts or early interruption of the examination prevented post-processing.

Determined cases

Morphometric evaluation

Significant differences were found in both P/M ($p < 0.001$) and MRPI ($p < 0.001$) with the multiple-group comparison. The distribution of morphometric data across diagnostic groups is represented in Figure 1 and Table 2.

Significant differences were confirmed for both P/M and MRPI on comparing PD/ PSP, PSP/MSA-c and PSP/MSA-p ($p < 0.01$). A significant difference was found for MRPI but not P/M in the comparison of PD and MSA-c ($p = 0.040$). Neither MRPI nor P/M was able to discriminate between PD and MSA-p ($p = 0.710$ and 0.685 , respectively).

In the comparison of PD and PSP, the effect of age as a covariate was significant for P/M ($p = 0.007$). No statistically significant differences related to gender were found.

Quantitative susceptibility mapping evaluation

The multiple-group comparison showed significant $\Delta\chi$ differences in the RN, STN and putamen ($p < 0.001$), SNImed, SNIlat, SNIIventr and SNIIint ($p < 0.05$) (Table 3). No significant differences were found in the SNII dors, pallidus and caudate.

The distribution of magnetic susceptibility data of the most significant ROIs across groups is represented in Figure 2. A pairwise comparison between PD and PSP showed significant $\Delta\chi$ differences in RN, SNImed, SNIlat, SNIIventr, SNIIint, STN and putamen ($p < 0.05$), confirmed after age correction. Comparing PD and MSA-p, significant $\Delta\chi$ differences were found in the putamen and RN

TABLE 1 Clinical and demographic details of determined and undetermined cases (median, IQR)

	PD ($n = 31$)	MSA-c ($n = 9$)	MSA-p ($n = 5$)	PSP ($n = 24$)	p value	Undetermined cases ($n = 42$)
Gender	24M/7F	7M/2F	4M, 1F	16 M, 8F	ns	26 M/16 F
Age (years)	62.0 (54.0–67.0)	59.0 (55.0–68.5)	64.0 (60.0–70.5)	73.5 (68.0–76.8)**	<0.001	71.0 (65.5–75.0)
Disease duration (years)	2.0 (1.0–7.0)	3.0 (1.5–3.5)	5.0 (3.5–5.0)	3.5 (3.0–5.0)	ns	3.0 (2.0–4.0)
UPDRS III	17 (11–25)	27 (19.5–31.5)	39 (32.5–45.5)	37 (25–42.5)**	<0.001	25 (16–31.5)
PSPRS	na	na	na	46 (40–54)	na	na
Main clinical features						
Rest tremor	16 (51%)	0	1 (20%)	3 (12.5%)		
Asymmetric parkinsonism	26 (84%)	4 (44%)	3 (60%)	13 (54%)		
Postural instability	5 (16%)	4 (44%)	3 (60%)	17 (71%)		
Orthostatic hypotension	3 (9%)	6 (67%)	4 (80%)	2 (8%)		
Urinary symptoms	4 (13%)	5 (56%)	5 (100%)	4 (17%)		

Abbreviations: F, female; IQR, interquartile range; M, male; MSA-c, multiple system atrophy cerebellar phenotype; MSA-p, multiple system atrophy parkinsonian phenotype; PD, Parkinson's disease; PSP, progressive supranuclear palsy; PSPRS, Progressive Supranuclear Palsy Rating Scale; UPDRS-III, subscore III of the Unified Parkinson's Disease Rating Scale.

** $p < 0.001$.

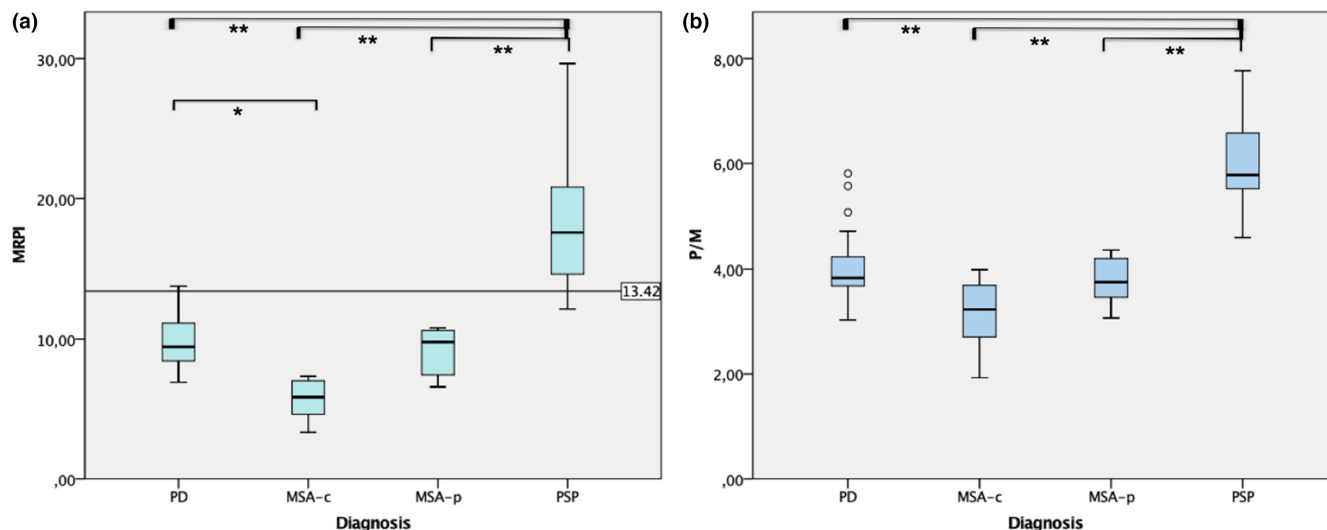


FIGURE 1 Distribution of morphometric data across diagnostic groups in the determined population. (a) MRPI results; the horizontal reference line corresponds to the MRPI optimal cut-off value 13.42 [22]. (b) P/M results. Pairwise comparisons between groups (after Bonferroni's correction; ** $p < 0.001$, * $p < 0.05$): MRPI, PD/PSP $p \leq 0.001$, MSA-c/PSP $p \leq 0.001$, MSA-p/PSP $p = 0.005$, MSA-c/PD $p = 0.040$; P/M, PD/PSP $p \leq 0.001$, MSA-c/PSP $p \leq 0.001$, MSA-p/PSP $p = 0.004$. MRPI, Magnetic Resonance Parkinsonism Index; MSA-c, multiple system atrophy cerebellar phenotype; MSA-p, multiple system atrophy parkinsonian phenotype; P/M, pons-to-midbrain ratio; PD, Parkinson's disease; PSP, progressive supranuclear palsy [Colour figure can be viewed at wileyonlinelibrary.com]

	PD (n = 31)	MSA-c (n = 5)	MSA-p (n = 9)	PSP (n = 24)	p value
MRPI	9.4 (8.4–11.2)	5.9 (4.6–7.1)	9.8 (7.0–10.7)	17.6 (14.4–21.0)**	<0.001
P/M	3.8 (3.7–4.3)	3.2 (2.6–3.8)	3.8 (3.3–4.3)	5.8 (5.5–6.6)**	<0.001

TABLE 2 Values of all MRPI and P/M measures in the different diagnostic groups of the determined population (expressed as median, IQR)

Abbreviations: IQR, interquartile range; MRPI, Magnetic Resonance Parkinsonism Index; MSA-c, multiple system atrophy cerebellar phenotype; MSA-p, multiple system atrophy parkinsonian phenotype; P/M, pons-to-midbrain ratio; PD, Parkinson's disease; PSP, progressive supranuclear palsy.

** $p < 0.001$.

($p < 0.05$). Significant $\Delta\chi$ differences comparing MSA-c and PSP were found in RN ($p < 0.01$). No significant differences were found comparing PD/MSA-c, MSA-p/PSP or MSA-p/MSA-c.

No statistically significant differences regarding gender were found.

Receiver operating characteristic curve analysis

The diagnostic accuracy of the main significant variables differentiating PD/PSP and PD/MSA-p was evaluated (Table 4). The accuracy of significant differences obtained comparing PD/MSA-c and PSP/MSA-c was not evaluated because all MSA-c cases were correctly diagnosed at baseline.

Definition of QSM diagnostic cut-off values

In the determined group, the distribution of susceptibility data in the boxplots of the most significant ROIs was visually explored (Figure 2), aiming to obtain QSM cut-off values capable of differentiating PD from both PSP and MSA-p (for this reason visual inspection was preferred to Youden's test), with optimal sensitivity or specificity.

$\Delta\chi$ of the RN showed excellent diagnostic accuracy in the comparison PD/PSP and good accuracy in the comparison PD/MSA-p. A very limited overlap between PD and both MSA-p and PSP was observed. The $\Delta\chi$ values of 100 and 130 ppb were defined as lower and upper cut-off values to differentiate PD from MSA-p and PSP cases, respectively, with maximum sensitivity (PD/MSA-p 100%, PD/PSP 100%) and specificity (PD/MSA-p 85%, PD/PSP 87%) (Figure 2a).

$\Delta\chi$ of the putamen provided optimal diagnostic accuracy in the comparison PD/MSA-p. Susceptibility values >100 ppb identified MSA-p cases with positive predictive value (PPV) 97%. $\Delta\chi$ of the putamen enabled the disentanglement of PD and PSP with good accuracy but with overlap between the two groups (Figure 2b).

$\Delta\chi$ of the STN differentiated PD from both PSP and MSA-p with good accuracy but the relevant overlap across groups prevented the definition of a diagnostic cut-off (Figure 2c).

$\Delta\chi$ of the SNImed failed to discriminate between PD and MSA-p but showed good diagnostic accuracy in the differential diagnosis PD/PSP, with maximum sensitivity (95%) for PSP of values >200 ppb (Figure 2d).

TABLE 3 $\Delta\chi$ values of all ROIs in the different diagnostic groups (expressed as median, IQR)

	PD	MSA-c	MSA-p	PSP	p value (Kruskal-Wallis test)
SNImed	196.1 (157.7–232.1)	210.6 (180.2–229.1)	235.7 (130.7–235.7)	247.7* (228.7–300.5)	0.003
SNIIlat	108.0 (89.0–134.7)	120.8 (89.2–149.3)	133.6 (80.4–133.6)	147.1* (112.1–186.9)	0.026
SNIIventr	123.5 (109.9–144.5)	149.6 (121.3–168.5)	184.6 (70.1–184.6)	191.7* (140.3–222.5)	0.004
SNIIint	158.3 (142.8–192.6)	170.5 (143.0–182.0)	204.3 (85.5–204.3)	205.3* (161.5–257.7)	0.032
SNII dors	139.2 (113.3–165.3)	130.8 (118.0–154.5)	153.8 (74.1–153.8)	168.1* (130.7–214.1)	0.013
RN	102.1 (86.6–120.1)	114.4 (98.7–117.3)	128.0 (118.2–128.0)	157.6** (127.1–176.8)	<0.001
STN	106.7 (88.8–128.6)	140.8 (116.3–148.2)	156.4 (126.5–156.4)	161.0** (120.9–188.4)	<0.001
Pallidus	89.3 (78.1–102.2)	98.2 (80.9–124.6)	66.0 (56.8–66.0)	96.4 (81.1–130.7)	ns
Putamen	61.3 (52.6–75.5)	76.1 (68.0–93.8)	114.1** (84.9–114.1)	91.0 (79.0–124.7)	<0.001
Caudate	45.6 (37.5–57.4)	52.2 (37.8–56.4)	53.8 (47.4–53.8)	61.5 (44.8–78.2)	ns

Abbreviations: $\Delta\chi$, magnetic susceptibility; IQR, interquartile range; MSA-c, multiple system atrophy cerebellar phenotype; MSA-p, multiple system atrophy parkinsonian phenotype; PD, Parkinson's disease; PSP, progressive supranuclear palsy; RN, red nucleus; ROI, region of interest; SNImed, medial part of substantia nigra at level I; SNII dors, SNIIint, SNIIventr, SNIIlat: dorsal, intermediate, ventral part of substantia nigra at level II; STN, subthalamic nucleus.

Undetermined cases

Evaluation of $\Delta\chi$ and application of QSM cut-off values in undetermined cases

The distribution of $\Delta\chi$ values in the RN, putamen and SNImed was explored in undetermined cases and the optimal $\Delta\chi$ cut-off values were applied (Figure 3).

$\Delta\chi$ of the RN showed significant differences between groups ($p = 0.007$; PD 103.8 ppb, IQR 82.9–118.2; MSA-p 125.6 ppb, IQR 107.3–149.1; PSP 150.6 ppb, IQR 104.8–177.4). The baseline $\Delta\chi$ of the RN enabled PD to be differentiated from PSP ($p = 0.005$) and PD from MSA-p ($p = 0.05$).

$\Delta\chi$ of the putamen did not show significant differences between diagnostic groups as a significant overlap was observed: PD 83.9 ppb, IQR 63.7–96.9; MSA-p 86.5 ppb, IQR 72.5–105.0; PSP 85.6 ppb, IQR 75.4–94.2. The $\Delta\chi$ of the putamen at baseline failed to discriminate PD from either PSP or MSA-p.

$\Delta\chi$ of the SNImed showed significant differences in the three-group comparison ($p = 0.030$): PD 187.1 ppb, IQR 145.1–213.8; MSA-p 187.7 ppb, IQR 158.4–221.0; PSP 239.0 ppb, IQR 202.1–256.4. The baseline $\Delta\chi$ of the SNImed allowed PD to be distinguished from PSP ($p = 0.038$) but failed to differentiate PD from MSA-p and MSA-p from PSP.

Diagnostic value was hypothesized for the RN cut-offs and, to a lesser extent, for the SNImed cut-off. Applying the RN lower cut-off (<100ppb), the final diagnosis was either PD ($n = 5$) or PSP ($n = 3$, two PSP-p, one PSP-v). No undetermined patients with a final diagnosis of MSA-p showed values below 100ppb at baseline. Using the $\Delta\chi$ RN upper cut-off (>130ppb), the final diagnosis was MSA-p ($n = 4$) or PSP ($n = 13$). No undetermined cases with a final diagnosis of PD showed RN values above 130ppb at baseline.

In undetermined cases with $\Delta\chi$ SNImed >200ppb at baseline, the final diagnosis was PD ($n = 6/38$, 16%), MSA-p ($n = 3/38$, 8%) or PSP ($n = 14/38$, 37%).

The putamen cut-off (100ppb) did not confirm diagnostic value in undetermined cases, even though significant differences were observed in the determined population, with high specificity for MSA-p. The role of disease duration was investigated as a possible confounding factor.

Disease duration did not differ between determined and undetermined cases, but it was close to the statistical significance threshold when including only MSA-p patients ($p = 0.061$). Considering both determined and undetermined cases, $\Delta\chi$ of the putamen was higher than 100ppb in 13% of patients with disease duration <3 years ($n = 57$; 25% of MSA-p, 26% of PSP) and in 26% of the remaining patients (50% of MSA-p, 27% of PSP). Conversely, in patients with disease duration <3 years, 95% of PSP and 100% of MSA-p patients had RN $\Delta\chi$ >100ppb, whereas 5% of cases with baseline values >130ppb had a final diagnosis of PD (Figure 4).

Diagnostic algorithm

As the MRPI value provided optimal diagnostic accuracy in differential diagnosis between PD/PSP and the QSM analysis revealed significant differences between PD and both PSP and MSA-p, it was attempted to improve the differential diagnosis of undetermined cases by including QSM information.

A diagnostic algorithm was applied combining the MRPI cut-off 13.42 [22] and the RN susceptibility cut-offs of our determined population (see Figure 5) to our undetermined cases. QSM was available in 39 undetermined cases: 13 PD, eight MSA-p, 18 PSP.

No undetermined case with a baseline MRPI >13.42 had a final diagnosis of MSA-p, as possible final diagnostic options were PSP ($n = 15$) or PD ($n = 2$). Applying the upper RN cut-off value to MRPI >13.42 cases it was possible to completely differentiate patients, as all subjects with RN $\Delta\chi$ >130ppb had a final diagnosis of PSP. In the remaining cases (MRPI > 13.42 and RN $\Delta\chi$ < 130ppb) a subsequent evaluation using $\Delta\chi$ of SNImed enabled a diagnosis of PSP to be excluded in subjects with baseline values <200ppb (not shown in Figure 5).

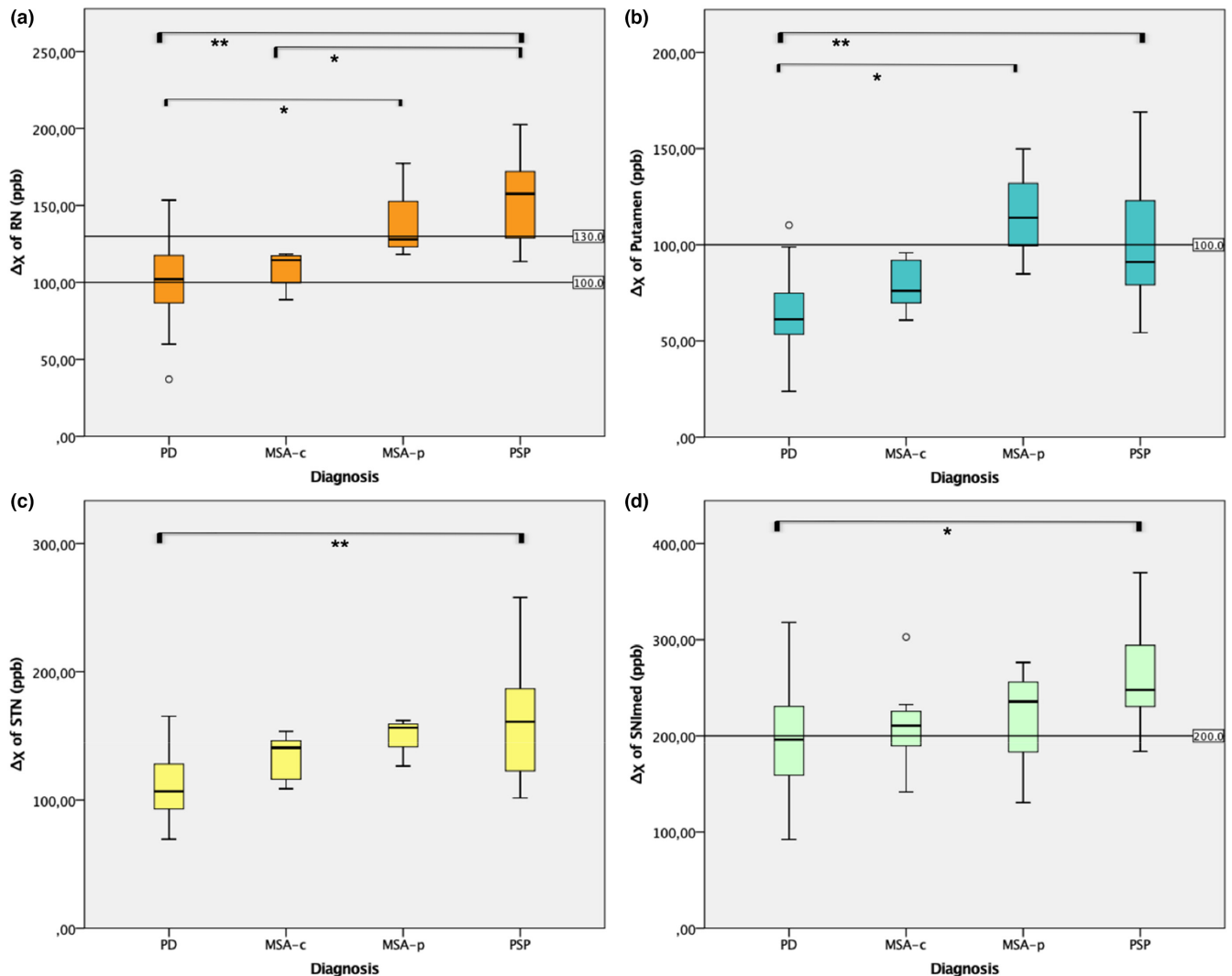


FIGURE 2 Distribution of $\Delta\chi$ in the most relevant ROIs across diagnostic groups in the determined population: (a) RN; (b) putamen; (c) STN; (d) SNImed. Horizontal reference lines correspond to the cut-off values of each ROI. RN, upper cut-off 130 ppb, lower cut-off 100 ppb; putamen, cut-off 100 ppb; SNImed, cut-off 200 ppb. Pairwise comparisons between groups (after Bonferroni's correction; $**p \leq 0.001$, $*p \leq 0.05$): RN, PD/PSP $p \leq 0.001$, MSA-c/PSP $p = 0.005$, PD/MSA-p $p = 0.048$; STN, PD/PSP $p \leq 0.001$; putamen, PD/PSP $p \leq 0.001$, PD/MSA-p $p = 0.033$; SNImed, PD/PSP $p = 0.002$. MSA-c, multiple system atrophy cerebellar phenotype; MSA-p, multiple system atrophy parkinsonian phenotype; PD, Parkinson's disease; PSP, progressive supranuclear palsy; RN, red nucleus; ROI, region of interest; SNImed, medial part of substantia nigra at level I; STN, subthalamic nucleus [Colour figure can be viewed at wileyonlinelibrary.com]

Undetermined cases with a baseline MRPI <13.42 had a final diagnosis of PD ($n = 11$), MSA-p ($n = 8$) or PSP (six, all not RS: five PSP-p, one PSP-v corticobasal syndrome). Applying the lower RN $\Delta\chi$ cut-off (<100 ppb), a final diagnosis of MSA-p could be excluded (four PD, one PSP-p). When the upper RN cut-off (>130 ppb) was applied to cases with MRPI <13.42 a final diagnosis of PD could be excluded (four MSA-p, one PSP-p). Further evaluation of SNImed $\Delta\chi$ in subjects with MRPI <13.42 and RN $\Delta\chi >130$ ppb excluded a PSP diagnosis in cases with baseline values <200 ppb (not shown in Figure 5).

The algorithm allowed the correct diagnostic classification of 17/26 undetermined atypical cases (13 PSP, four MSA-p). To evaluate the diagnostic value of the algorithm in MSA-c cases, the morphometric and QSM cut-offs were applied to the entire population.

As expected, all MSA-c cases had an MRPI <13.42 whereas RN $\Delta\chi$ was <130 ppb.

DISCUSSION

In this study morphometric and QSM MRI techniques were combined to evaluate the potential of regional atrophy and iron deposition as in vivo diagnostic biomarkers of degenerative parkinsonisms. The application of other advanced MRI techniques (e.g., diffusion and neuromelanin imaging) as a support to clinical evaluation has provided encouraging results [51]. The use of diffusion tensor imaging first supported classification of subjects diagnosed with PD, atypical parkinsonism and essential tremor, and distinguished them from

TABLE 4 Diagnostic accuracy of the main significant variables differentiating PD/PSP and PD/MSA-p

Variable PD/PSP	AUC (<i>p</i> value)	95% CI	Variable PD/MSA-p	AUC (<i>p</i> value)	95% CI
MRPI	0.976 (<i>p</i> < 0.001)	0.939–1	MRPI	ns (<i>p</i> = 0.923)	–
P/M	0.956 (<i>p</i> < 0.001)	0.900–1	P/M	ns (<i>p</i> = 0.698)	–
$\Delta\chi$ RN	0.942 (<i>p</i> < 0.001)	0.872–1	$\Delta\chi$ RN	0.862 (<i>p</i> = 0.016)	0.708–1
$\Delta\chi$ putamen	0.889 (<i>p</i> < 0.001)	0.774–1	$\Delta\chi$ putamen	0.954 (<i>p</i> = 0.011)	0.863–1
$\Delta\chi$ STN	0.844 (<i>p</i> < 0.001)	0.713–0.974	$\Delta\chi$ STN	0.885 (<i>p</i> = 0.030)	0.728–1
$\Delta\chi$ SNImed	0.854 (<i>p</i> < 0.001)	0.740–0.968	$\Delta\chi$ SNImed	ns (<i>p</i> = 0.628)	–

Abbreviations: $\Delta\chi$, magnetic susceptibility; AUC, area under the curve; CI, confidence interval; MRPI, Magnetic Resonance Parkinsonism Index; MSA-p, multiple system atrophy parkinsonian phenotype; PD, Parkinson's disease; P/M, pons-to-midbrain ratio; PSP, progressive supranuclear palsy; RN, red nucleus; SNImed, medial part of substantia nigra at level I; STN, subthalamic nucleus.

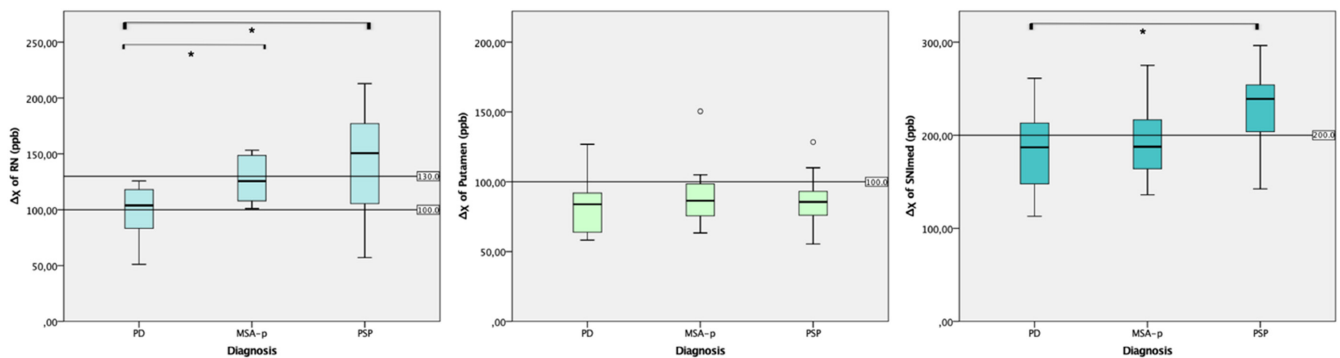


FIGURE 3 Distribution of $\Delta\chi$ of RN (left), putamen (middle) and SNImed (right) across diagnostic groups in undetermined cases. Horizontal lines correspond to the cut-off values. Pairwise comparisons between groups after Bonferroni's correction; **p* < 0.05. RN, upper cut-off 130 ppb, lower cut-off 100 ppb; putamen, cut-off 100 ppb; SNImed, cut-off 200 ppb. RN, red nucleus, SNImed, medial part of substantia nigra at level I [Colour figure can be viewed at wileyonlinelibrary.com]

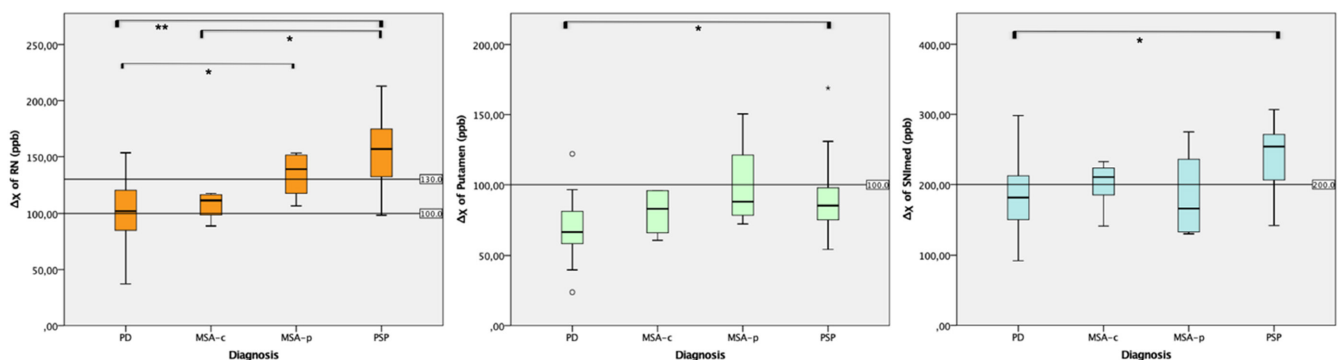


FIGURE 4 Distribution of $\Delta\chi$ of RN (left), putamen (middle) and SNImed (right) across diagnostic groups considering determined and undetermined cases with disease duration < 3 years. Horizontal lines correspond to the cut-off values. Pairwise comparisons between groups after Bonferroni's correction; **p* < 0.05. Putamen, cut-off 100 ppb; RN, upper cut-off 130 ppb, lower cut-off 100 ppb; SNImed, cut-off 200 ppb. RN, red nucleus; SNImed, medial part of substantia nigra at level I [Colour figure can be viewed at wileyonlinelibrary.com]

control subjects [52]. Subsequent use of diffusion MRI along with the Movement Disorders Society UPDRS part III improved differential diagnosis of PD and atypical parkinsonisms in a large cohort of subjects [53]. Similar results were recently obtained with other techniques such as neurite orientation dispersion and density imaging and free-water imaging [54]. Automated analysis of mean diffusivity of the middle cerebellar peduncles and putamen was reported to provide excellent diagnostic accuracy to discriminate patients with

MSA from PD in the early to moderate disease stages [55]. Besides the single MRI techniques, the application of multimodal protocols (e.g., T1-weighted/T2-weighted ratio and voxel-based morphometry [56]) was hypothesized to further improve differential diagnosis between PD and atypical parkinsonisms [57].

Our results first highlighted the importance of the clinical evaluation, with high specificity but suboptimal sensitivity of PD, MSA and PSP diagnostic criteria, as in all determined cases (62%) baseline

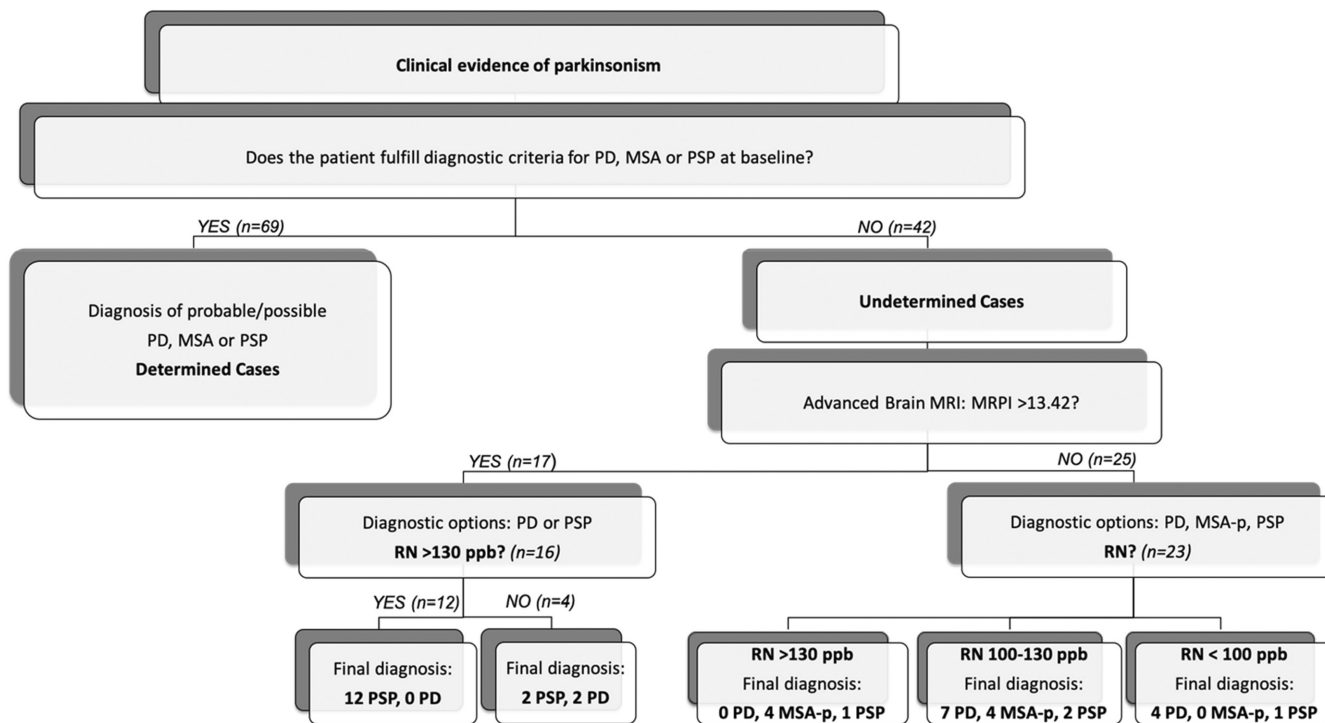


FIGURE 5 Diagnostic algorithm representing the design of the study and diagnostic classification of undetermined cases according to morphometric and QSM cut-offs. DD, differential diagnosis; MRPI, Magnetic Resonance Parkinsonism Index; MSA-p, parkinsonian phenotype of multiple system atrophy; PD, Parkinson's disease; PSP, progressive supranuclear palsy; QSM, quantitative susceptibility mapping; RN, red nucleus

diagnosis was confirmed. In our population PSP or MSA-p were found as PD mimics at baseline, whereas all MSA-c cases were correctly diagnosed.

Both the morphometric indices investigated confirmed optimal diagnostic accuracy in the differential diagnosis between PD and PSP but failed to discriminate PD from MSA-p. In our determined population diagnostic accuracy of MRPI was found to be slightly superior to P/M and not affected by age, even if time-consuming.

As previously reported [33–35], $\Delta\chi$ values in a few nigral and extranigral ROIs of PD patients were significantly different from those of PSP and MSA-p cases. Diagnostic accuracy comparing PD and PSP ranged from good (putamen, SNImed and STN) to optimal (RN), and the latter was similar to that of the morphometric indices.

Disease-specific diagnostic cut-offs for parkinsonian disorders are currently under investigation, with few reports regarding the globus pallidus and putamen [34, 43]. After prospective evaluation of our determined cases QSM cut-offs were defined for the RN, putamen and medial part of the SN, previously reported to have diagnostic potential to discriminate PD from atypical cases [33, 35].

The cut-offs were applied to undetermined cases and the magnetic susceptibility of RN appeared as a promising diagnostic biomarker. In particular, the lower RN cut-off provided 100% sensitivity for MSA-p whereas the upper cut-off improved identification of atypical cases (MSA-p and PSP). The SNImed cut-off provided mild additional diagnostic value, with high sensitivity for PSP cases. In contrast, $\Delta\chi$ of the putamen did not confirm its potential as a diagnostic biomarker, at least in the early disease stages. Our observations

supported the hypothesis of a later increase of putaminal $\Delta\chi$ in the disease course of MSA-p, discouraging its use as an early radiological biomarker, even if it could be evaluated as a staging and progression biomarker. In contrast, an early involvement of RN was hypothesized in atypical cases.

These observations support the value of QSM in the diagnostic workup of suspected parkinsonism. Of note, the diagnostic accuracy of both QSM and morphometric methods could have been affected by the high percentage of PSP-RS (67%) and by the low number of MSA-p in the determined population. Neuroanatomical differences across the PSP phenotypes have recently been noted, but a high tau burden was demonstrated in the RN and midbrain structures across all variants [18]. Lesser RN pathological involvement was reported in PSP-p and PSP-v (speech language and pure gait freezing) and could explain the reduced sensitivity of the QSM method in a minority of cases, as in our study.

In our undetermined cases an algorithm was evaluated combining the MRPI cut-off 13.42, highly specific for PSP also early in the disease course, with the RN susceptibility cut-offs validated in our determined population (Figure 5); in a minority of uncertain cases the SNImed susceptibility cut-off was further applied. According to our results a combination of the two techniques could improve differential diagnosis between PD, PSP and MSA-p, possibly since the early phases. Indeed, differences in the distribution of RN $\Delta\chi$ across diagnostic groups were confirmed with the post hoc analysis in patients with disease duration up to 3 years (Figure 3). Both the morphometric and the quantitative values obtained in our population

are comparable to previous studies using similar methodological approaches and including similar disease groups and healthy subjects. The accuracy of this multimodal evaluation could be improved by using fully automated [22] and new morphometric measures [14, 58], designed to improve detection of all PSP phenotypes.

Our study has a few limitations. One is the lack of pathological confirmation; however, the longitudinal design of the study should have limited possible diagnostic inaccuracy. Another possible limitation could be the absence of a control group; nevertheless, the main aim of our study was to discriminate between patients with clinically defined parkinsonism and both the morphometric and quantitative susceptibility values obtained in our population reflect the results of previous studies including similar disease groups and healthy subjects. Whilst the complexity of the MRI protocol, acquisition times and post-processing, might be considered a further limitation, the main purpose of our multimodal protocol is currently academic, aiming to improve the selection of patients for clinical trials. Automated QSM processing routes, as for MRPI, could enable a wide use of the tool, possibly targeting midbrain structures to limit acquisition and processing times. The reproducibility of our measures at a broader level could be a further limitation, considering the variability of QSM methodology across centres [59]. The definition of the most appropriate RR remains a crucial point and a wide heterogeneity across studies was reported [59]. In most cases, the cerebrospinal fluid or white matter, as in this study, was used, whilst other authors referenced their QSM data to other brain regions or avoided the use of a reference region [59]. To test the RR impact, our analysis was repeated using unreferenced data and the overall results were confirmed. Taking these considerations into account, our observations require to be validated in larger multicentre studies.

In conclusion, the use of a diagnostic multimodal MRI protocol for degenerative parkinsonisms, including both morphometric and quantitative iron-sensitive techniques, could improve differential diagnosis between PD and its main mimics, PSP and MSA-p.

AUTHOR CONTRIBUTIONS

Sonia Mazzucchi: Data curation (lead); formal analysis (supporting); investigation (lead); writing – original draft (lead). **Eleonora Del Prete:** Data curation (supporting); investigation (equal); writing – review and editing (equal). **Mauro Costagli:** Conceptualization (equal); investigation (equal); project administration (equal); software (lead); supervision (equal); writing – review and editing (equal). **Daniela Frosini:** Conceptualization (equal); investigation (supporting); supervision (equal); writing – review and editing (supporting). **Davide Paoli:** Data curation (supporting); investigation (equal); writing – review and editing (supporting). **Gianmichele Migaleddu:** Conceptualization (equal); investigation (equal); methodology (equal); software (equal); writing – review and editing (supporting). **Paolo Cecchi:** Data curation (equal); investigation (supporting); project administration (equal); software (equal); writing – review and editing (supporting). **Graziella Donatelli:** Conceptualization (equal); project administration (equal); supervision (supporting); writing – review and editing (equal). **Riccardo Morganti:** Formal analysis (equal); methodology (equal); supervision; writing

– review and editing. **Gabriele Siciliano:** Project administration; supervision; writing – review and editing. **Mirco Cosottini:** Conceptualization (equal); methodology (equal); project administration (equal); resources (equal); supervision; writing – review and editing. **Roberto Ceravolo:** Conceptualization (equal); project administration (equal); resources (equal); supervision; writing – review and editing.

ACKNOWLEDGEMENT

Open Access Funding provided by Universita degli Studi di Pisa within the CRUI-CARE Agreement.

CONFLICT OF INTEREST

All authors report no financial disclosures or conflict of interest related to the content of this research. Roberto Ceravolo reports receiving honoraria from Abbvie, Zambon, Lusofarmaco, UCB and General Electric. All other authors have no disclosures to report.

DATA AVAILABILITY STATEMENT

The data that support the findings of this study are available from the corresponding author upon reasonable request.

ORCID

Graziella Donatelli  <https://orcid.org/0000-0002-5325-0746>

Roberto Ceravolo  <https://orcid.org/0000-0003-1412-9406>

REFERENCES

1. Postuma RB, Berg D, Stern M, et al. MDS clinical diagnostic criteria for Parkinson's disease. *Mov Disord.* 2015;30(12):1591-1601. doi:10.1002/mds.26424
2. Gilman S, Wenning GK, Low PA, et al. Second consensus statement on the diagnosis of multiple system atrophy. *Neurology.* 2008;71(9):670-676. doi:10.1212/01.wnl.0000324625.00404.15
3. Höglinger GU, Respondek G, Stamelou M, et al. Clinical diagnosis of progressive supranuclear palsy: the Movement Disorder Society criteria. *Mov Disord.* 2017;32(6):853-864. doi:10.1002/mds.26987
4. Poewe W, Seppi K, Tanner CM, et al. Parkinson disease. *Nat Rev Dis Primers.* 2017;3:17013. doi:10.1038/nrdp.2017.13
5. Chougar L, Pyatigorskaya N, Degos B, Grabli D, Lehéryc S. The role of magnetic resonance imaging for the diagnosis of atypical parkinsonism. *Front Neurol.* 2020;17(11):665. doi:10.3389/fneur.2020.00665
6. Heim B, Krismer F, De Marzi R, et al. Magnetic resonance imaging for the diagnosis of Parkinson's disease. *J Neural Transm (Vienna).* 2017;124(8):915-964. doi:10.1007/s00702-017-1717-8
7. Cosottini M, Ceravolo R, Faggioni L, et al. Assessment of midbrain atrophy in patients with progressive supranuclear palsy with routine magnetic resonance imaging. *Acta Neurol Scand.* 2007;116(1):37-42. doi:10.1111/j.1600-0404.2006.00767.x
8. Oba H, Yagishita A, Terada H, et al. New and reliable MRI diagnosis for progressive supranuclear palsy. *Neurology.* 2005;64:2050-2055. doi:10.1212/01.WNL.0000165960.04422.D0
9. Kato N, Arai K, Hattori T. Study of the rostral midbrain atrophy in progressive supranuclear palsy. *J Neurol Sci.* 2003;210:57-60. doi:10.1016/s0022-510x(03)00014-5
10. Quattrone A, Nicoletti G, Messina D, et al. MR imaging index for differentiation of progressive supranuclear palsy from Parkinson disease and the Parkinson variant of multiple system atrophy. *Radiology.* 2008;246(1):214-221. doi:10.1148/radiol.2453061703

11. Zanigni S, Calandra-Buonaura G, Manners DN, et al. Accuracy of MR markers for differentiating progressive supranuclear palsy from Parkinson's disease. *Neuroimage Clin*. 2016;11:736-742. doi:10.1016/j.nicl.2016.05.016
12. Mangesius S, Hussl A, Krismer F, et al. MR planimetry in neurodegenerative parkinsonism yields high diagnostic accuracy for PSP. *Parkinsonism Relat Disord*. 2018;46:47-55. doi:10.1016/j.parkreldis.2017.10.020
13. Morelli M, Arabia G, Novellino F, Salsone M, Giofre L, Condino F, Messina D, Quattrone A MRI measurements predict PSP in unclassifiable parkinsonisms: a cohort study. *Neurology* 2011;13;77(11):1042-1047. doi:10.1212/WNL.0b013e31822e55d0
14. Heim B, Mangesius S, Krismer F, et al. Diagnostic accuracy of MR planimetry in clinically unclassifiable parkinsonism. *Parkinsonism Relat Disord*. 2021;82:87-91. doi:10.1016/j.parkreldis.2020.11
15. Whitwell JL, Höglinger GU, Antonini A, et al. Radiological biomarkers for diagnosis in PSP: where are we and where do we need to be? *Mov Disord*. 2017;32(7):955-971. doi:10.1002/mds.27038
16. Longoni G, Agosta F, Kostic VS, et al. MRI measurements of brainstem structures in patients with Richardson's syndrome, progressive supranuclear palsy-parkinsonism, and Parkinson's disease. *Mov Disord*. 2011;26(2):247-255. doi:10.1002/mds.23293
17. Massey LA, Micallef C, Paviour DC, et al. Conventional magnetic resonance imaging in confirmed progressive supranuclear palsy and multiple system atrophy: cMRI in PSP and MSA. *Mov Disord*. 2012;27(14):1754-1762. doi:10.1002/mds.24968
18. Whitwell JL, Tosakulwong N, Botha H, et al. Brain volume and flortaucipir analysis of progressive supranuclear palsy clinical variants. *Neuroimage Clin*. 2020;25:102152. doi:10.1016/j.nicl.2019.102152
19. Grijalva RM, Trang Thu Pham N, Huang Q, et al. Brainstem biomarkers of clinical variant and pathology in progressive supranuclear palsy. *Mov Disord*. 2021;37:702-712. doi:10.1002/mds.28901
20. Seongken K, Chong Hyun S, Woo Hyun S, et al. Diagnostic performance of the magnetic resonance parkinsonism index in differentiating progressive supranuclear palsy from Parkinson's disease: an updated systematic review and meta-analysis. *Diagnostics (Basel)*. 2021;12(1):12. doi:10.3390/diagnostics12010012
21. Picillo M, Tepedino MF, Abate F, et al. Midbrain MRI assessments in progressive supranuclear palsy subtypes. *J Neurol Neurosurg Psychiatry*. 2020;91(1):98-103. doi:10.1136/jnnp-2019-321354
22. Nigro S, Antonini A, Vaillancourt DE, et al. Automated MRI classification in progressive supranuclear palsy: a large international cohort study. *Mov Disord*. 2020;35(6):976-983. doi:10.1002/mds.28007
23. Heim B, Krismer F, Seppi K. Differentiating PSP from MSA using MR planimetric measurements: a systematic review and meta-analysis. *J Neural Transm (Vienna)*. 2021;128(10):1497-1505. doi:10.1007/s00702-021-02362-8
24. Morelli M, Arabia G, Messina D, et al. Effect of aging on magnetic resonance measures differentiating progressive supranuclear palsy from Parkinson's disease. *Mov Disord*. 2014;29(4):488-495. doi:10.1002/mds.25821
25. Mangesius S, Hussl A, Tagwercher S, et al. No effect of age, gender and total intracranial volume on brainstem MR planimetric measurements. *Eur Radiol*. 2020;30(5):2802-2808. doi:10.1007/s00330-019-06504-1
26. Blazejewska AI, Schwarz ST, Pitiot A, et al. Visualization of nigrosome 1 and its loss in PD pathoanatomical correlation and in vivo 7 T MRI. *Neurology*. 2013;81(6):534-540. doi:10.1212/WNL.0b013e31829e6fd2
27. Cosottini M, Frosini D, Pesaresi I, et al. MR imaging of the substantia nigra at 7 T enables diagnosis of Parkinson disease. *Radiology*. 2014;271(3):831-838. doi:10.1148/radiol.14131448
28. Schwarz ST, Afzal M, Morgan PS, et al. The 'swallow tail' appearance of the healthy nigrosome—a new accurate test of Parkinson's disease: a case-control and retrospective cross-sectional MRI study at 3 T. Bush AI, editor. *PLoS ONE*. 2014;9(4):e93814. doi:10.1371/journal.pone.0093814
29. Cosottini M, Frosini D, Pesaresi I, et al. Comparison of 3 T and 7 T susceptibility-weighted angiography of the substantia nigra in diagnosing Parkinson disease. *Am J Neuroradiol*. 2015;36(3):461-466. doi:10.3174/ajnr.A4158
30. Mahlknecht P, Krismer F, Poewe W, Seppi K. Meta-analysis of dorsolateral nigral hyperintensity on magnetic resonance imaging as a marker for Parkinson's disease: DNH on MRI as a marker for PD. *Mov Disord*. 2017;32(4):619-623. doi:10.1002/mds.26932
31. Reiter E, Mueller C, Pinter B, et al. Dorsolateral nigral hyperintensity on 3.0 T susceptibility-weighted imaging in neurodegenerative parkinsonism. *Mov Disord*. 2015;30(8):1068-1076. doi:10.1002/mds.26171
32. Frosini D, Ceravolo R, Tosetti M, Bonuccelli U, Cosottini M. Nigral involvement in atypical parkinsonisms: evidence from a pilot study with ultra-high field MRI. *J Neural Transm*. 2016;123(5):509-513. doi:10.1007/s00702-016-1529-2
33. Sjöström H, Granberg T, Westman E, Svenningsson P. Quantitative susceptibility mapping differentiates between parkinsonian disorders. *Parkinsonism Relat Disord*. 2017;44:51-57. doi:10.1016/j.parkreldis.2017.08.029
34. Ito K, Ohtsuka C, Yoshioka K, et al. Differential diagnosis of parkinsonism by a combined use of diffusion kurtosis imaging and quantitative susceptibility mapping. *Neuroradiology*. 2017;59(8):759-769. doi:10.1007/s00234-017-1870-7
35. Mazzucchi S, Frosini D, Costagli M, et al. Quantitative susceptibility mapping in atypical parkinsonisms. *Neuroimage Clin*. 2019;24:101999. doi:10.1016/j.nicl.2019.101999
36. Beliveau V, Nørgaard M, Birkl C, Seppi K, Scherfler C. Automated segmentation of deep brain nuclei using convolutional neural networks and susceptibility weighted imaging. *Hum Brain Mapp*. 2021;42(15):4809-4822. doi:10.1002/hbm.25604
37. Barbosa JHO, Santos AC, Tumas V, et al. Quantifying brain iron deposition in patients with Parkinson's disease using quantitative susceptibility mapping, R2 and R2*. *Magn Reson Imaging*. 2015;33(5):559-565. doi:10.1016/j.mri.2015.02.021
38. Murakami Y, Kakeda S, Watanabe K, et al. Usefulness of quantitative susceptibility mapping for the diagnosis of Parkinson disease. *Am J Neuroradiol*. 2015;36(6):1102-1108. doi:10.3174/ajnr.A4260
39. Langkammer C, Pirpamer L, Seiler S, et al. Quantitative susceptibility mapping in Parkinson's disease. *PLoS One*. 2016;11(9):e0162460. doi:10.1371/journal.pone.0162460
40. Guan X, Xuan M, Gu Q, et al. Regionally progressive accumulation of iron in Parkinson's disease as measured by quantitative susceptibility mapping. *MR Biomed*. 2017;30(4):e3489. doi:10.1002/nbm.3489
41. Acosta-Cabronero J, Cardenas-Blanco A, Betts MJ, et al. The whole-brain pattern of magnetic susceptibility perturbations in Parkinson's disease. *Brain*. 2017;140(1):118-131. doi:10.1093/brain/aww278
42. Pyatigorskaya N, Sanz-Morère CB, Gaurav R, et al. Iron imaging as a diagnostic tool for Parkinson's disease: a systematic review and meta-analysis. *Front Neurol*. 2020;11:366. doi:10.3389/fneur.2020.00366
43. Azuma M, Hirai T, Nakaura T, et al. Combining quantitative susceptibility mapping to the morphometric index in differentiating between progressive supranuclear palsy and Parkinson's disease. *J Neurol Sci*. 2019;406:116443. doi:10.1016/j.jns.2019.116443
44. Jellinger KA, Seppi K, Wenning GK. Grading of neuropathology in multiple system atrophy: proposal for a novel scale. *Mov Disord*. 2005;20(Suppl 12):S29-S36. doi:10.1002/mds.20537
45. Grimm MJ, Respondek J, Stamelou KM, et al. How to apply the Movement Disorder Society criteria for diagnosis of progressive

- supranuclear palsy. *Mov Disord.* 2019;34(8):1228-1232. doi:10.1002/mds.27666
46. Fahn S, Elton RL. Unified Parkinson's Disease Rating Scale. In: Fahn S, Marsden CD, Calne D, Goldstein M, eds. *Recent Developments in Parkinson's Disease.* MacMillan Healthcare Information; 1987:153-163.
47. Golbe LI, Ohman-Strickland PA. A clinical rating scale for progressive supranuclear palsy. *Brain.* 2007;130:1552-1565. doi:10.1093/brain/awm032
48. Jankovic J, McDermott M, Carter J, et al. Variable expression of Parkinson's disease: a base-line analysis of the DATA TOP cohort. *Neurology.* 1990;40(10):1529-1534.
49. Berg D, Adler CH, Bloem BR, et al. Movement Disorder Society criteria for clinically established early Parkinson's disease. *Mov Disord.* 2018;33(10):1643-1646. doi:10.1002/mds.27431
50. Lancione M, Donatelli G, Cecchi P, Cosottini M, Tosetti M, Costagli M. Echo-time dependency of quantitative susceptibility mapping reproducibility at different magnetic field strengths. *Neuroimage.* 2019;197:557-564. doi:10.1016/j.neuroimage.2019.05.004
51. Peralta C, Strafella AP, van Eimeren T, et al. Pragmatic approach on neuroimaging techniques for the differential diagnosis of parkinsonisms. *Mov Disord Clin Prac.* 2021;9(1):6-19. doi:10.1002/mdc3.13354
52. Prodoehl J, Li H, Planetta PJ, et al. Diffusion tensor imaging of Parkinson's disease, atypical parkinsonism, and essential tremor. *Mov Disord.* 2013;28(13):1816-1822. doi:10.1002/mds.25491
53. Archer DB, Bricker JT, Chu WT, et al. Development and validation of the automated imaging differentiation in parkinsonism (AID-P): a multi-site machine learning study. *Lancet Digit Health.* 2019;1(5):e222-e231. doi:10.1016/s2589-7500(19)30105-0
54. Mitchell T, Archer DB, Chu WT, et al. Neurite orientation dispersion and density imaging (NODDI) and free-water imaging in parkinsonism. *Hum Brain Mapp.* 2019;40(17):5094-5107. doi:10.1002/hbm.24760
55. Krismer F, Beliveau V, Seppi K, et al. Automated analysis of diffusion-weighted magnetic resonance imaging for the differential diagnosis of multiple system atrophy from Parkinson's disease. *Mov Disord.* 2021;36(1):241-245. doi:10.1002/mds.28281
56. Ponticorvo S, Manara R, Russillo MC, et al. Magnetic resonance T1w/T2w ratio and voxel-based morphometry in multiple system atrophy. *Sci Rep.* 2021;11(1):21683. doi:10.1038/s41598-021-01222-5
57. Arribarat G, De Barros A, Péran P. Modern brainstem MRI techniques for the diagnosis of Parkinson's disease and parkinsonisms. *Front Neurol.* 2020;11:791. doi:10.3389/fneur.2020.00791
58. Quattrone A, Morelli M, Nigro S, et al. A new MR imaging index for differentiation of progressive supranuclear palsy-parkinsonism from Parkinson's disease. *Parkinsonism Relat Disord.* 2018;54:3-8. doi:10.1016/j.parkreldis.2018.07.016
59. Ravanfar P, Loi SM, Syeda WT, et al. Systematic review: quantitative susceptibility mapping (QSM) of brain iron profile in neurodegenerative diseases. *Front Neurosci.* 2021;15:618435. doi:10.3389/fnins.2021.618435

SUPPORTING INFORMATION

Additional supporting information can be found online in the Supporting Information section at the end of this article.

How to cite this article: Mazzucchi S, Del Prete E, Costagli M, et al. Morphometric imaging and quantitative susceptibility mapping as complementary tools in the diagnosis of parkinsonisms. *Eur J Neurol.* 2022;29:2944-2955. doi: [10.1111/ene.15447](https://doi.org/10.1111/ene.15447)